Is ENSO an Adequate Analogue for Tropical Pacific Climate Change?

Pedro DiNezio[1*]
Amy Clement[1]
Gabriel Vecchi[2]

*pdinezio@rsmas.miami.edu

[1]University of Miami/RSMAS
[2]NOAA/GFDL

ABSTRACT

El Niño/Southern Oscillation (ENSO) has often been invoked as physical framework for interpreting changes in the tropical Pacific for both future and past climate changes. The interpretation is as follows: If an external forcing introduces some east-west asymmetry in the equatorial Pacific, this asymmetry will be amplified, in the same way as interannual perturbations are, through the Bjerknes feedback.

Here we present two physical aspects of the equatorial response to external forcing that render this analogy inadequate to project or communicate impacts associated with Global Warming (GW), attribute changes in the modern observations, or interpret paleoclimatic proxies of the Last Glacial Maximum (LGM).

We show that this analogy has limitations arising from basic physics of the ocean response to wind changes and from the response of the Walker Circulation to changes in the global hydrological cycle. These physical processes result in a weaker Bjerknes feedback for GW or the LGM compared with ENSO, and consequently the climate response does not become El Niño- or La Niña-like.

1. THERMOCLINE RESPONSE

In contrast with ENSO, when the thermocline response to changes in the trade winds is dominated by changes in the thermocline tilt (Figure 1a), on longer time scales, the thermocline response to weaker winds consists of a zonal mean shoaling in response to the curl of the wind, in addition to the relaxation of the thermocline tilt (Figure 1b).

Unlike ENSO, the coupling between wind and SST changes in the eastern equatorial Pacific is much weaker because the zonal mean shoaling of the equatorial thermocline opposes the deepening due to a reduced tilt.

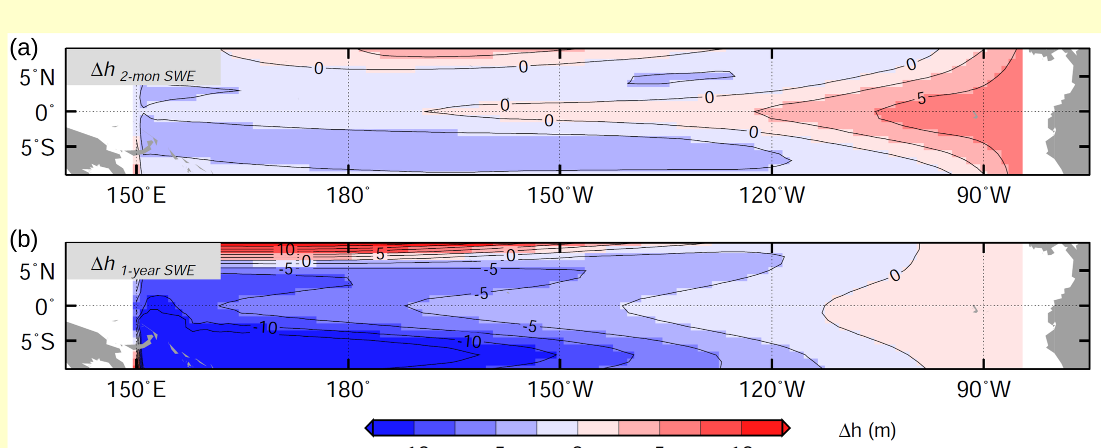

Figure 1 – Thermocline depth changes after **(a)** two months and **(b)** one year simulated by a 1 ½ layer shallow-water type model in response to weaker winds. The wind changes are derived from the multimodel-mean changes simulated by the IPCC AR4 GCMs in response to 2xCO2 (SRESA1B experiment).

The changes simulated by the GCM experiments used in the IPCC AR4 are consistent with this dynamical argument, showing a shoaling of the thermocline throughout the equatorial Pacific in response to 2xCO2 (Figure 2).

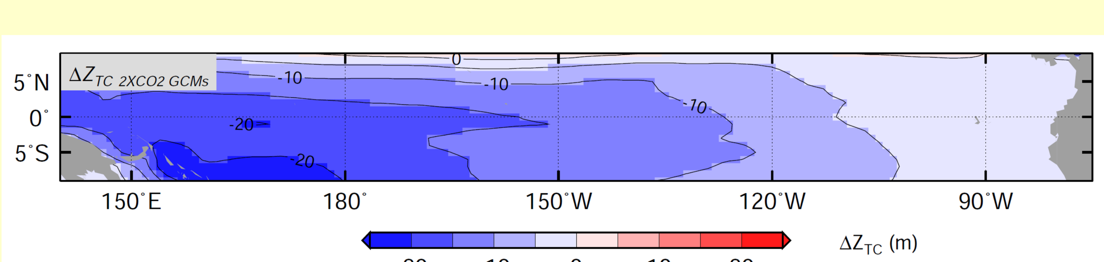

Figure 2 – Multimodel-mean changes in thermocline depth simulated the IPCC AR4 GCMs in response to 2xCO2 (SRESA1B experiment).

The GCM experiments also project an increase in the sharpness of the thermocline, which cannot be explained by dynamical processes, but is consistent with a response to local and remote buoyancy forcing. **This increased stratification enhances ocean dynamical cooling in eastern equatorial Pacific 'putting a break' on SST growth, i.e. the ocean dynamical thermostat. This is in contrast to an El Niño event when the thermocline changes are heavily dominated by a reduced east-west tilt, which leads to ocean dynamical heating and SST growth, i.e. the Bjerknes feedback.** Hence, even though the trade winds weaken during GW, the thermocline response drives an SST change that is opposite to El Niño.

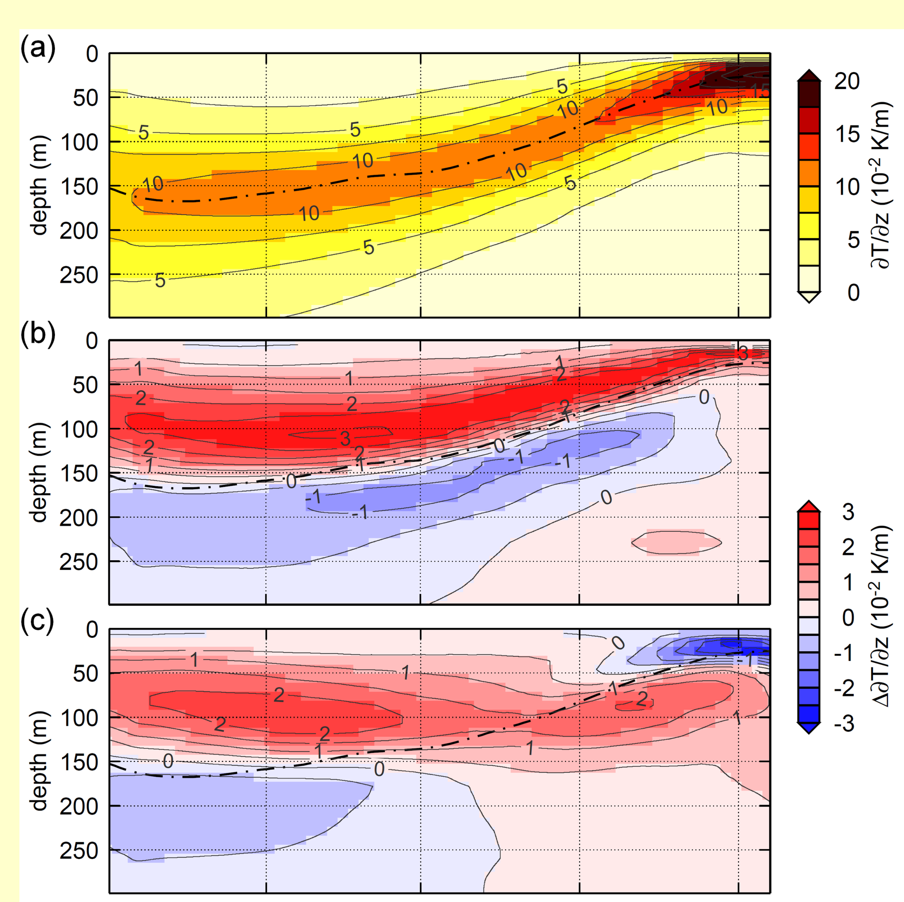

Figure 3 – (a) Multimodel vertical temperature gradient at the equator (i.e. the thermocline) simulated by 20+ GCMs participating in the IPCC AR4 (20C3M experiment). **(b)** Response of the vertical temperature gradient to Global Warming (GW) simulated in the SRESA1B experiment. **(c)** Multi-model anomaly in vertical temperature gradient averaged from composite El Niño events simulated by each of the GCMs in the 20C3M experiment. All panels correspond to an equatorial band between 5°S and 5°N. The dash-dotted line is the depth of the thermocline in the multi-model control.

2. WALKER CIRCULATION

Unlike during El Niño events, when a weaker Walker circulation is accompanied by a reduced east-west SST contrast, the majority of GCMs used for the IPCC AR4 simulate a weakening of the east-west sea level pressure (SLP) gradient accompanied by changes in the east-west SST gradient that can be of either sign (Figure 4, red dots).

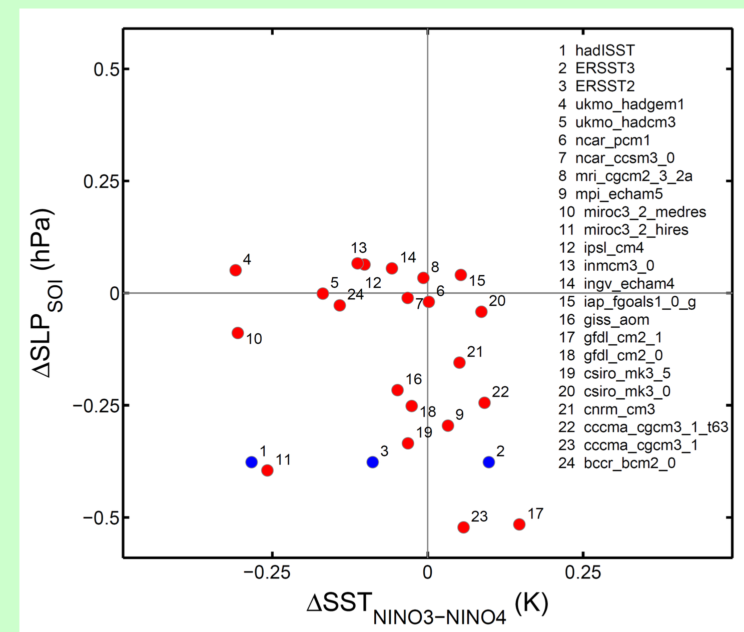

Figure 4 – Change in sea surface temperature (SST) and sea level pressure (SLP) gradient along the equator in observational datasets (blue) and model projections for the 1900 to 2004 period (red).

The SST gradient is computed as the difference between a NINO3 (5°S–5°N, 150°W–90°W) and a NINO4 region (5°S–5°N, 160°E–150°W). The SLP gradient is a measure of the strength of the Walker circulation and is computed as the area-average SLP change between a "Tahiti" region (150°W–90°W, 10°S–10°N) minus a "Darwin" region (100°E–180°, 10°S–10°N). The model projections correspond to the 20C3M and SRESA1B experiments used in the IPCC AR4.

While SLP and SST gradients are tightly linked on ENSO time scales, under GW, the weakening of the Walker circulation results also from constrains in the hydrological cycle that are independent from the zonal SST gradient (Vecchi and Soden, 2007). This mechanism also explains the apparent contradiction between SST and SLP gradients in some of the observational reconstructions (Figure 4, blue dots).

IMPLICATIONS FOR INTERPRETING PROXIES

These ideas can also be applied to reconstructions of the climate of the Last Glacial Maximum (LGM), where both El Niño and La Niña analogies have been made. Proxies based on foraminifera transfer functions suggest a stronger zonal SST gradient and a stronger thermocline tilt, while Mg/Ca ratios in foraminifera suggest either a weaker or unaltered zonal SST gradient. GCM experiments also simulate a wide range of responses, from weaker to stronger SST gradient.

However, all models simulate a *deeper* thermocline, and a *stronger* Walker circulation. Hence, just like in the case of GW, there can be significant ocean and atmospheric changes without robust changes in the zonal SST gradient.

Moreover, GCM simulations of the LGM show a prominent interhemispheric asymmetry (Figure 5), characterized by strong cross-equatorial winds in response to high-latitude forcing, in addition to **stronger** trade winds. The ocean response to the meridional asymmetry is expected to depart further from ENSO in the LGM than during GW, making the analogy even less adequate. From these arguments it is clear that proxies of the ocean thermal structure or trade wind strength would be better suited than the zonal SST gradient to constrain our understanding of the physical processes operating in the tropics during the LGM.

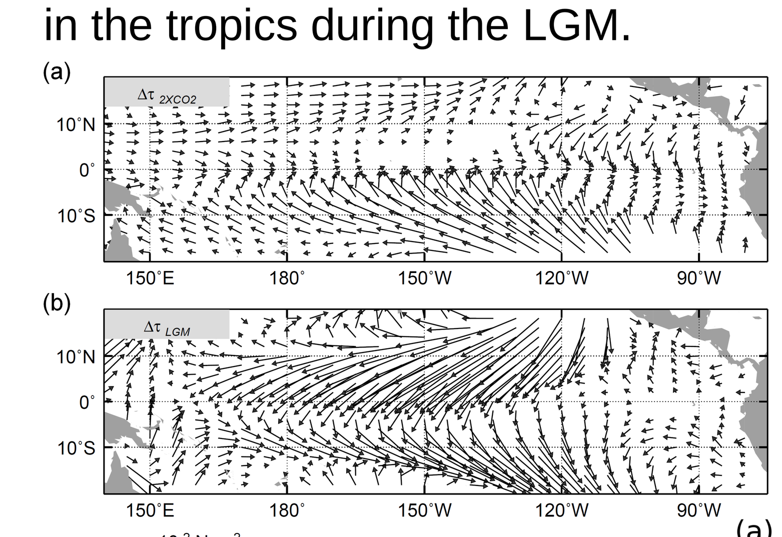

Figure 5 – Multi-model change in surface wind stress in response to **(a)** doubling of CO2 (2XCO2) and **(b)** LGM boundary conditions simulated by five GCMs participating in both CMIP3 and PMIP2 (UK Met Office HadCM3, NCAR CCSM3.0, MIROC 3.2 medres, IAP FGOALS v1.0g, CNRM CM3)

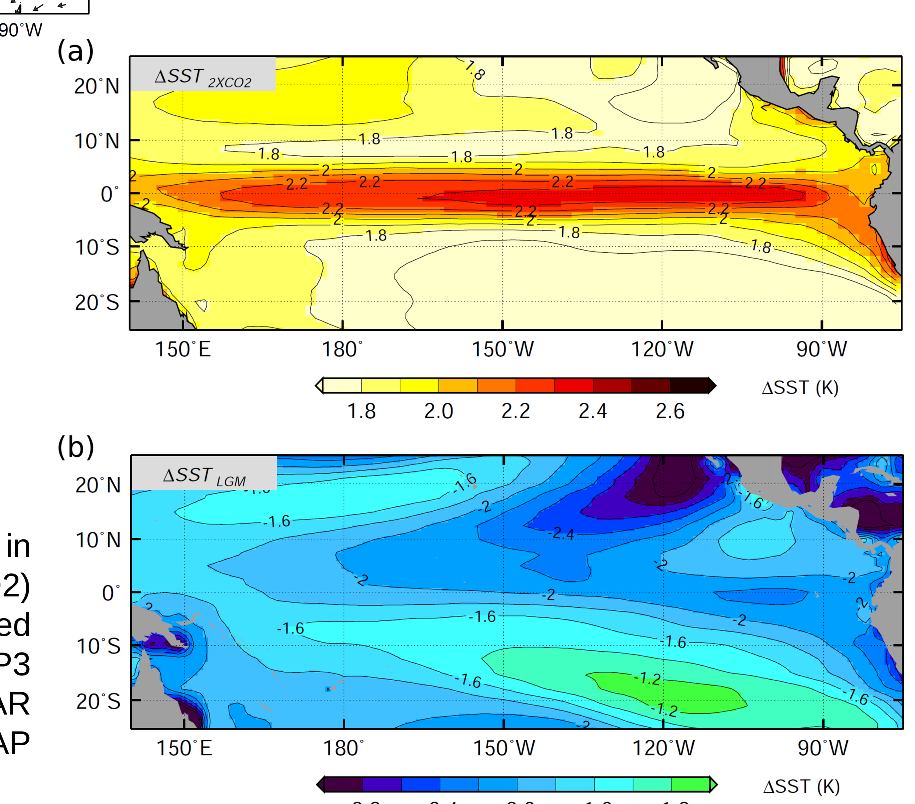

Figure 6 – Multi-model SST change in response to **(a)** doubling of CO2 (2XCO2) and **(b)** LGM boundary conditions simulated by five GCMs participating in both CMIP3 and PMIP2 (UK Met Office HadCM3, NCAR CCSM3.0, MIROC 3.2 medres, IAP FGOALS v1.0g, CNRM CM3)

To conclude, the physical processes operating on long-term climate change allow for a less rigid relationship between SSTs, thermocline, and trade winds. As result of the much weaker Bjerknes feedback, the signature of the SST changes does not need to be El Niño- or La Niña-like. For instance, the enhanced equatorial warming simulated in the GW experiments (Figure 6a) results from changes in advection in response to weaker trade winds, instead of changes in the thermocline tilt. In the LGM experiments the SST response departs further from ENSO, showing a clear interhemispheric asymmetry that results from changes in ocean advection driven by the anomalous cross-equatorial winds. In both cases, the thermocline changes oppose the atmospheric forcing according to ocean dynamical thermostat mechanism.

ACKNOWLEDGEMENTS This work was made possible by the international modeling groups participating in the CMIP3 and PMIP2 projects. NSF grant 0500275 and NOAA grant NA0604310142 funded this study. We are thankful to M. Cane and B. Kirtman for their insight into the equatorial adjustment problem.